Atg16L1 deficiency confers protection from uropathogenic *Escherichia coli* infection in vivo

Caihong Wang[a,1], Graziella R. Mendonsa[a,1], Jane W. Symington[a,1], Qunyuan Zhang[b], Ken Cadwell[c,2], Herbert W. Virgin[c,d], and Indira U. Mysorekar[a,c,3]

Departments of [a]Obstetrics and Gynecology, [b]Genetics, and [c]Pathology and Immunology, and [d]Midwest Regional Center of Excellence for Biodefense and Emerging Infectious Diseases Research, Washington University School of Medicine, St. Louis, MO 63110

Edited* by Roy Curtiss III, Arizona State University, Tempe, AZ, and approved May 22, 2012 (received for review March 7, 2012)

Urinary tract infection (UTI), a frequent and important disease in humans, is primarily caused by uropathogenic *Escherichia coli* (UPEC). UPEC forms acute cytoplasmic biofilms within superficial urothelial cells and can persist by establishing membrane-enclosed latent reservoirs to seed recurrent UTI. The host responds with an influx of innate immune cells and shedding of infected epithelial cells. The autophagy gene *ATG16L1* has a commonly occurring mutation that is associated with inflammatory disease and intestinal cell abnormalities in mice and humans. Here, we show that Atg16L1-deficient mice (Atg16L1^{HM}) cleared bacteriuria more rapidly and thoroughly than controls and showed rapid epithelial recovery. Atg16L1 deficiency was associated with a potent proinflammatory cytokine response with increased recruitment of monocytes and neutrophils to infected bladders. Chimeric and genetic studies showed that Atg16L1^{HM} hematopoietic cells alone could increase clearance and that Atg16L1-deficient innate immune cells were required and sufficient for enhanced bacteriuric clearance. We also show that Atg16L1-deficient mice exhibit cell-autonomous architectural aberrations of superficial urothelial cells, including increases in multivesicular bodies, lysosomes, and expression of the UPEC receptor Up1a. Finally, we show that Atg16L1^{HM} epithelial cells contained a significantly reduced number of latent reservoirs. Together, our results show that Atg16L1 deficiency confers protection in vivo to the host against both acute and latent UPEC infection, suggest that deficiency in a key autophagy protein can be protective against infection in an animal model of one of the most common diseases of women worldwide, and may have significant clinical implications for understanding the etiology of recurrent UTIs.

Atg5 | Lyz-Cre | Rag1

Macroautophagy (henceforth, autophagy) is a well-conserved cellular pathway required to maintain cellular homeostasis, recycle cellular components, and eliminate intracellular pathogens (1, 2). In response to nutrient deprivation, stress, or other signals, double membrane-bound autophagosomes are recruited to envelop bulk cytoplasm, damaged organelles, large cytoplasmic protein aggregates, or invading pathogens. These autophagosomes then fuse with lysosomes, and therefore, their cargo may be degraded. Autophagy genes and proteins play a multiplicity of roles in both innate and adaptive immunity (3–5). For example, in mice deficient for Atg5 in macrophages and neutrophils, there is increased susceptibility to infection with *Listeria monocytogenes* and *Toxoplasma gondii*, and Atg5 deficiency is associated with decreased resistance to viral encephalitis (6, 7). Pathogens have also evolved sophisticated mechanisms to evade or subvert the host autophagy machinery for survival and persistence within cells (8) by blocking the xenophagic degradation of intracellular pathogens or the function of autophagy in innate and adaptive immunity. Although most work to date shows that autophagy as a whole and specific autophagy proteins are detrimental to the microorganism, they may also have proviral or probacterial effects. For example, autophagosomes may serve as a protected niche for intracellular bacteria and/or source of nutrients for intracellular pathogens (9). In vivo evidence of such a propathogen role of autophagy is still lacking.

The autophagy gene/protein Atg16L1 plays a key role in autophagosome maturation as part of a protein complex that directs the microtubule-associated protein light chain 3 (LC3) to autophagosomes en route to their fusion with lysosomes (1, 10). We previously showed that mice deficient in Atg16L1 (Atg16L1^{HM}) display reduced autophagy. In addition, they develop, on viral infection, intestinal abnormalities similar to pathologies found in Crohn's disease patients, including abnormalities in the integrity, architecture, and function of Paneth cells, which are specialized secretory epithelial cells of the small intestine (11, 12). Atg16L1 has also been shown to play a role in modulating proinflammatory responses in mice and humans (13, 14). Furthermore, population genetic studies have positively associated a common polymorphism in the *ATG16L1* gene with inflammatory bowel disease (15, 16). One explanation for a high prevalence of such harmful gene variants would be protection from common infections. However, such a protective role for mutation of an autophagy gene has not been reported.

Here, we use Atg16L1^{HM} mice as a genetically tractable model to determine whether mutation in an autophagy gene can increase resistance to a common infection. Urinary tract infections (UTIs), primarily caused by uropathogenic *Escherichia coli* (UPEC), are among the most common infectious diseases in humans, resulting in an estimated 13 million outpatient visits yearly in the United States (17). Recurrent UTIs are a serious problem, with ~25% of patients experiencing multiple episodes per year despite appropriate antibiotic treatment and absence of bacteriuria between episodes (18). In an in vivo mouse model, UPEC invades bladder superficial cells by binding uroplakin receptors expressed on the cell surface (19, 20). During the acute stage of infection (0–72 h), intracellular UPEC replicates rapidly and establishes cytoplasmic biofilms termed intracellular bacterial communities (IBCs) in bladders of both mice and humans (21, 22). Major mechanisms for control of UPEC-induced UTI include exfoliation of the superficial epithelial cell layer containing IBCs into the urine and influx of innate immune cells (23–26). However, despite the innate immune host response, a subset of UPEC still survives and establishes long-term reservoirs within urothelial cells, termed quiescent intracellular reservoirs (QIRs) (27), which are enclosed within vesicles decorated with late endosomal/lysosomal markers. Latent UPEC within QIRs can reemerge to seed recurrent UTIs likely through cAMP-regulated exocytic processes to reenter the bladder lumen concomitant with urothelial regeneration (27–29).

Results

Atg16L1 Deficiency Leads to Superficial Cell Architectural Abnormalities. To determine if Atg16L1 plays a role in UPEC invasion and persistence within the bladder, we first examined the morphology

Author contributions: C.W., G.R.M., J.W.S., and I.U.M. designed research; C.W., G.R.M., and J.W.S. performed research; C.W., G.R.M., J.W.S., and Q.Z. analyzed data; and C.W., G.R.M., J.W.S., K.C., H.W.V., and I.U.M. wrote the paper.

The authors declare no conflict of interest.

*This Direct Submission article had a prearranged editor.

[1]C.W., G.R.M., and J.W.S. contributed equally to this work.

[2]Present address: Skirball Institute of Biomolecular Medicine, Department of Microbiology, New York University School of Medicine, New York, NY 10016.

[3]To whom correspondence should be addressed. E-mail: indira@wustl.edu.

This article contains supporting information online at www.pnas.org/lookup/suppl/doi:10.1073/pnas.1203952109/-/DCSupplemental.

of superficial urothelial cells, the target cells for UPEC invasion, in Atg16L1^{HM} mice. These cells are highly specialized to rapidly expand and shrink as the bladder fills and contracts, and this function requires large plaques of hexagonal arrays of uroplakin protein complexes, which are transported by discoidal fusiform vesicles (FVs) and multivesicular bodies (MVBs) to maintain cellular architecture and barrier properties (30, 31). UPEC uses the uroplakins (Up1a) as receptors to facilitate invasion and entry into these urothelial cells (30–32). We reasoned that Atg16L1 deficiency might alter this membranous intracellular network, because changes in intracellular membranes associated with granule exocytosis are observed in the intestinal Paneth cell in Atg16L1^{HM} mice (11). Here, we show that Atg16L1 deficiency governs urothelial cell architecture as follows. First, bladders of Atg16L1^{HM} mice exhibited decreased (by 78%) Atg16L1 expression (Fig. S1). Second, superficial epithelial cells of uninfected Atg16L1^{HM} mice showed dramatic accumulation of vesicles (Fig. 1*B*) compared with those cells of control (WT) mice (Fig. 1*A*). Transmission EM (TEM) confirmed this vesicular congestion (Fig. 1 *C–F* and Fig. S2 *A–C*) and revealed significantly greater numbers of organelles with the morphology of MVBs and lysosomes in Atg16L1^{HM} superficial cells (Fig. 1 *G* and *H*) ($P < 0.05$ and $P < 0.01$, respectively). Third, given that this vesicular system is responsible for uroplakin transport and recycling and that disruption in vesicular trafficking of FVs and MVBs is associated with aberrant MVB accumulation (28, 30, 33), we next determined the effect of Atg16L1 deficiency on uroplakin receptor expression. We found increased Up1a expression in Atg16L1^{HM} bladders (Fig. 1 *I* and *J*), correlating with the increased MVBs seen by TEM in Atg16L1^{HM} superficial cells. These data show that Atg16L1 is a key player in modulating and/or maintaining the proper architecture of superficial cells, including membranes that are involved in uroplakin expression.

Autophagy Machinery Intersects with UPEC. The autophagy pathway functions to sequester intracellular pathogens after cellular invasion through recognition and decoration by LC3 and an adaptor protein p62 (1, 9, 34, 35). To determine whether such autophagy-associated pathogen recognition is engaged on UPEC infection in vivo, we infected bladders of adult female WT mice by transurethral inoculation of a clinical cystitis isolate UTI89 (36). On UPEC invasion of bladder superficial cells, Atg16L1 and LC3 puncta colocalized with UPEC within IBCs at 6 h postinoculation (hpi) and QIRs at 14 d postinoculation (dpi) (Fig. S3 *A–D* and *A–D Insets*). p62 puncta, normally present throughout the urothelium in an uninfected state (Fig. S3*E*), were recruited to the site of bacterial entry (Fig. S3*F*). Thus, autophagy proteins associate with UPEC during the acute and latent stages of UPEC pathogenesis in vivo.

Atg16L1 Deficiency Leads to Rapid Clearance of Bacteriuria and Significant Reduction in Latent Reservoirs. To determine if Atg16L1 deficiency-induced alterations in superficial urothelial cell morphology and increased uroplakin expression affect UPEC invasion and persistence in superficial urothelial cells, we induced a UTI in adult female control and Atg16L1^{HM} mice. The progress of UPEC-induced UTI was monitored by measuring shedding of bacteria into the urine (i.e., bacteriuria), analyzing bacterial invasion and colonization in the bladder tissue, and evaluating the number of QIRs. We found that UPEC invaded and colonized the bladders of Atg16L1^{HM} and control mice during the acute infection stage (6 hpi) at similar levels (Fig. 2 *A* and *B*). Strikingly, however, as early as 1 dpi, Atg16L1^{HM} mice exhibit significantly reduced bacteriuria (Fig. 2*A*) and bladder tissue UPEC titers (Fig. 2*B*), and thus, they were more effective at clearing bacteriuria than controls ($P < 0.01$). We also show that this enhanced bacteriuric clearance can be induced even in the presence of one hypomorphic *Atg16L1* allele: Atg16L1^{HM} heterozygote mice expressing 41% of Atg16L1 protein (Fig. S1) cleared UPEC faster compared with control mice by 3 dpi ($P < 0.05$) (Fig. S4). Thus, the presence of a single hypomorphic *Atg16L1* allele is sufficient to confer protection from bacterial infection.

Given the abnormal accumulation of MVBs in the superficial bladder epithelial cells of Atg16L1^{HM} mice, we investigated whether these epithelial changes were altering early invasion events, leading to the decreased bacterial burden. Examination at 6 hpi for IBC formation (Fig. 2*C*) showed similar numbers of IBCs in Atg16L1^{HM} and control bladders (Fig. 2*D*), consistent with similar urine and

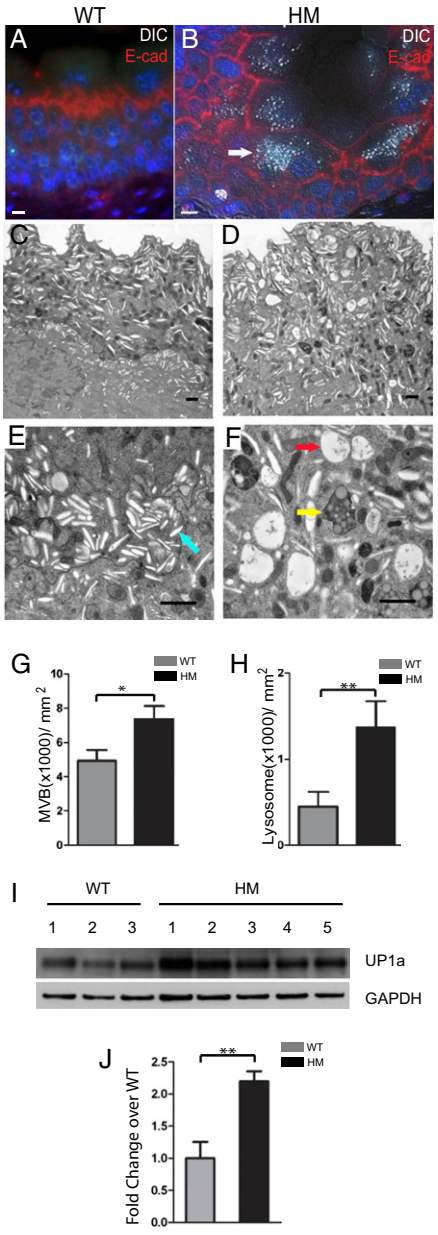

Fig. 1. Atg16L1 deficiency leads to superficial cell architectural abnormalities. (*A* and *B*) Immunofluorescence and differential interference contrast (DIC) imaging analysis showing (*A*) WT and (*B*) Atg16L1^{HM} (HM) urothelium depicting enhanced vesicular congestion in HM (cyan, arrow). E-cadherin (red) outlines urothelial cells; nuclei are blue with biz-benzimide. (Scale bar: 10 μm.) (*C* and *D*) TEM showing WT (*C*) and HM (*D*) superficial cell ultrastructure confirming architectural changes in HM urothelium. Panels representative of 10- to 15-μm^2 regions examined in three mice. (Scale bar: 1 μm.) (*E* and *F*) High magnification image of WT (*E*) and HM (*F*) superficial cells displaying fusiform vesicles (FVs; blue arrow), multivesicular bodies (MVBs; red arrow), and lysosomes (LYs; yellow arrow). (Scale bar: 1 μm.) (*G* and *H*) Quantification of MVBs (*G*) and lysosomes (*H*) showing a significant increase in HM urothelium. Bars represent mean ± SEM. *$P < 0.05$, **$P < 0.01$ by unpaired two-tailed *t* test. (*I* and *J*) Western blot (*I*) of whole-bladder protein indicates increased UP1a in HM mice relative to WT mouse (normalized to GAPDH) and quantification of UP1a expression relative to WT (*J*). Bars represent mean ± SEM. **$P < 0.01$ by unpaired two-tailed *t* test.

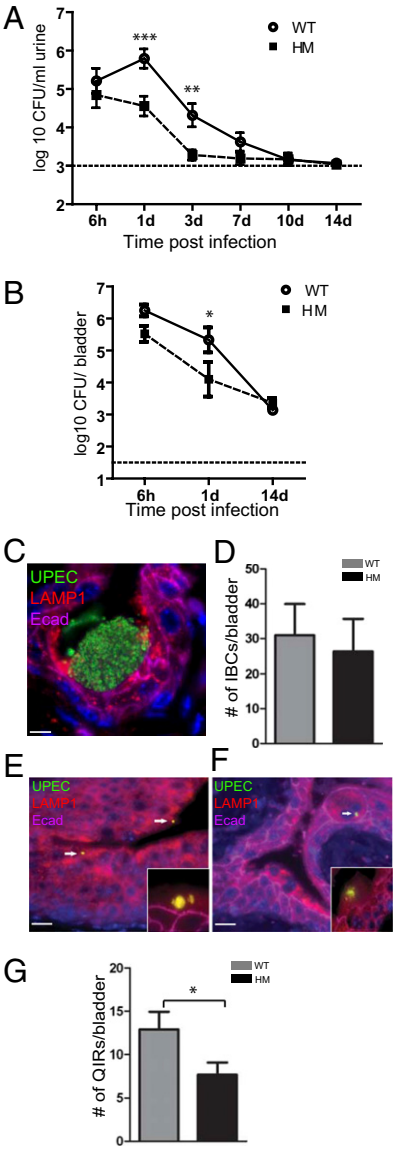

Fig. 2. Atg16L1 deficiency leads to rapid clearance of bacteriuria, acute reduction in bladder colonization, and significant reduction of latent UPEC reservoirs. (*A*) CFU counts of bacteriuria plotted as mean ± SEM of the log10 value at 6 hpi to 14 dpi showing rapid reductions of bacteriuria in HM mice 1 dpi and clearance by 3 dpi. $n = 5$–15 mice per time point per genotype; $n = 3$ experiments. $^{**}P < 0.01$, $^{***}P < 0.001$ by two-way ANOVA with Bonferroni posttest. (*B*) CFU counts from full bladder homogenates show similar titers in the HM and WT mice at 6 hpi and significantly lower levels in HM mice by 1 dpi. $n = 3$–5 mice per time point per genotype; $n = 3$ experiments. $^{*}P < 0.05$ by two-way ANOVA with Bonferroni posttest. (*C*) IF analysis of HM bladders at 6 hpi with UPEC showing normal IBC formation. (*D*) Quantification of IBCs in WT vs. HM bladders at 6 hpi. (*E* and *F*) IF analysis of WT (*E*) and HM bladders (*F*) at 14 dpi with UPEC showing QIRs (green, arrows). *E Inset* and *F Inset* show higher magnification images of a bacterial QIR enclosed by Lamp1 staining (red). E-cadherin (purple) outlines urothelial cells; nuclei are blue with biz-benzimide. (*G*) Quantification of QIRs in WT vs. HM bladders at 14 dpi indicating a significant decrease in QIR numbers in HM mice. $n = 6$ sections/bladder, $n = 38$–55 mice/genotype. (Scale bar: 10 μm.) $^{*}P < 0.05$ by unpaired two-tailed *t* test.

bladder bacteria titers at 6 hpi. Thus, decreased Atg16L1 expression in Atg16L1^{HM} bladders is associated with decreased bacteriuria, which is not caused by alteration of early epithelial invasion and colonization events.

We next examined control and Atg16L1^{HM} bladders at 14 dpi to determine if enhanced acute clearance of bacteriuria from the bladders of Atg16L1^{HM} mice was associated with reduced establishment of QIRs. QIRs can seed recurrent infection, although the reservoirs contain relatively small numbers of bacteria that are often at or below detection levels in urine and bladder cfu titers (27). We found that bladders of Atg16L1^{HM} mice harbored significantly reduced numbers of Lamp1+ QIRs compared with bladders of control mice (Fig. 2 *E*–*G*) ($P < 0.05$). Thus, Atg16L1 deficiency resulted in increased resistance to the formation of protected niches containing UPEC during the latent stage of infection. Together, our data show that Atg16L1 deficiency is associated with decreased bacteriuria and bladder colonization by UPEC at acute stages of infection and protection from UPEC latency.

Superficial Urothelial Cell Regeneration Is Hastened in Atg16L1-Deficient Bladders. Urothelial tissue regeneration is an important step in the resolution of UTIs (37). We analyzed bladder tissue sections from control and Atg16L1^{HM} mice at 6 and 14 dpi and found that, relative to uninfected bladders from control and Atg16L1^{HM} mice (Fig. S5 *A* and *B*), the bladders of control mice at 6 dpi displayed persistent stromal inflammation and proliferating transitional epithelial cells (Fig. S5*C*, arrow). In contrast, Atg16L1^{HM} bladders displayed newly regenerated, terminally differentiated, and nonproliferating superficial cells (Fig. S5*D*, arrow) and resolution of inflammation (Fig. S5*D*). By 14 dpi, both control and Atg16L1^{HM} bladders displayed regenerated superficial cells (Fig. S5 *E* and *F*), but bladders of control mice continued to show inflammation (Fig. S5*E*, arrowheads). The proliferative index of stem/progenitor cells after infection was similar between control and Atg16L1^{HM} mice at 6 dpi (Fig. S5*G*), suggesting that the stem cell niche was unaffected by Atg16L1 deficiency. However, by 14 dpi, although continued proliferative activity was observed in bladders of control mice (Fig. S5*E*, arrow), it had returned to basal levels in bladders of Atg16L1^{HM} mice (Fig. S5 *F* and *H*) ($P < 0.05$). Thus, early bacterial clearance in Atg16L1^{HM} mice correlated with faster epithelial recovery. Interestingly, TEM analysis of WT and Atg16L1^{HM} bladders at 14 dpi (Fig. S6) confirmed that the regenerated superficial cells in Atg16L1^{HM} bladders also exhibited the ultrastructural vesicular defects observed before infection, suggesting Atg16L1 deficiency-induced cellular abnormality in superficial cells was autonomous to this cell type.

Atg16L1 Deficiency in the Hematopoietic Compartment Contributes Significantly to Clearance of Bacterial Load. We next sought to determine the cellular mechanisms underlying the enhanced clearance of bacteria in Atg16L1^{HM} bladders and the resulting host-protective outcome. Previous work has shown that both hematopoietic and epithelial compartments are required to mount an efficient host response to UPEC infection in the bladder (24). Although Atg16L1 deficiency in the epithelial compartment affected latent UPEC reservoir establishment, it did not show any differences in acute infection events (e.g., in IBC formation) that could explain the more rapid clearance in Atg16L1^{HM} mice. Furthermore, Atg16L1 plays a role in modulating proinflammatory responses (5, 13, 14). We reasoned, therefore, that Atg16L1 deficiency in immune cells could contribute to UPEC clearance directly by a potent proinflammatory response or indirectly by inducing the aberrant superficial urothelial cell architecture.

To elucidate contributions of Atg16L1 deficiency in hematopoietic cells to clearance of UTI, we generated reciprocal bone marrow chimera (Fig. 3 *A*–*D*). To examine the contribution of the Atg16L1 hypomorphic hematopoietic compartment, we compared WT recipients receiving Atg16L1^{HM} bone marrow with those recipients receiving WT bone marrow. We show that WT mice receiving Atg16L1^{HM} bone marrow cleared bacteriuria faster: significantly more complete clearance was evident at 7 and 14 dpi as indicated by the lower bacteriuria titers in the presence of Atg16L1^{HM} bone marrow (Fig. 3*E*). Differential interference contrast (DIC) imaging and TEM analysis revealed no aberrant changes in the epithelium of these WT animals, suggesting that Atg16L1^{HM} hematopoietic cells do not contribute to the

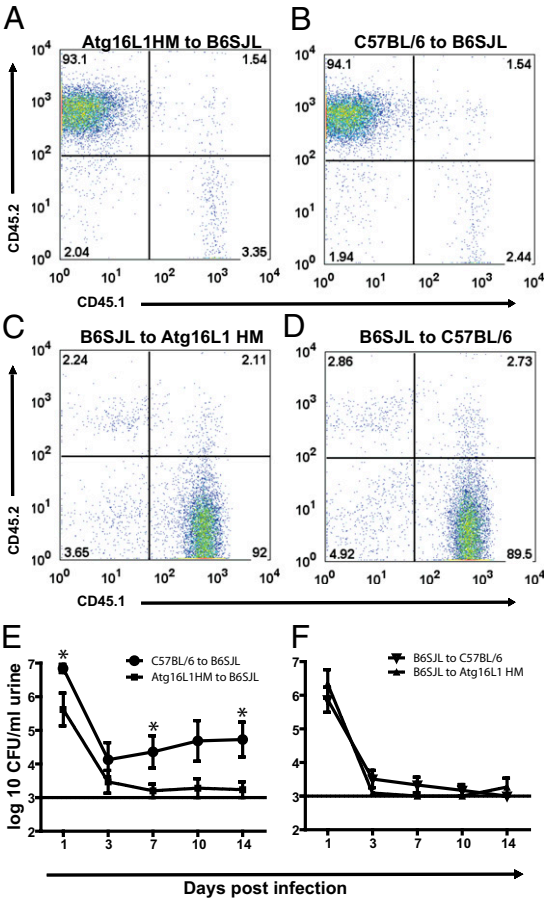

Fig. 3. Atg16L1 deficiency in the hematopoietic compartment leads to increased bacteriuric clearance. (*A–D*) Flow cytometric analysis of splenocytes showed effective engraftment of donor bone marrow for each bone marrow chimera animal. (*E*) Urinary UPEC cfu counts at 1–14 dpi indicating more rapid and thorough clearance of bacteria in the B6SJL mice receiving Atg16L1^{HM} bone marrow compared with those mice receiving WT bone marrow. n = 5–10 mice per time point per genotype; n = 2 experiments. *P < 0.05 by two-way ANOVA with Bonferroni posttest. (*F*) Urinary UPEC cfu counts at 1–14 dpi showing similar UPEC clearance in WT mice and Atg16L1^{HM} mice receiving B6SJL bone marrow. n = 5–10 mice per time point per genotype; n = 2 experiments.

superficial epithelial cell abnormalities (Fig. S7), consistent with those abnormalities being cell autonomous; however, the presence of Atg16L1^{HM} bone marrow alone is sufficient for faster clearance of UTI infection.

Next, we sought to determine if Atg16L1 deficiency in the epithelium would contribute to the bacteriuric clearance and compared mice with WT and Atg16L1^{HM} epithelium receiving WT bone marrow. As expected, urothelial architectural abnormalities similar to those abnormalities described in Atg16L1^{HM} mice were observed in the bladders of Atg16L1^{HM} recipients receiving WT bone marrow (Fig. S7); however, these mice did not display faster clearance of bacteriuria (Fig. 3*F*). Our findings indicate that the Atg16L1-deficient hematopoietic compartment is necessary for the clearance, that Atg16L1 deficiency in the epithelium alone with a WT hematopoietic compartment is not sufficient for faster luminal clearance, and that Atg16L1 deficiency-induced epithelial architectural abnormality is not regulated by Atg16L1 deficiency in hematopoietic cells.

Atg16L1 Deficiency in the Innate Immune Compartment Is Necessary and Sufficient for Bacteriuric Clearance. Autophagy protein deficiency can have substantial effects on the adaptive and innate immune system (1). Thus, we sought to determine whether lymphocytes contributed to the UPEC pathogenesis phenotypes observed in Atg16L1^{HM} mice. We bred Atg16L1^{HM} mice onto a Rag1$^{-/-}$ background, which is T cell- and B cell-deficient (38) (henceforth termed Rag1$^{-/-}$/Atg16L1^{HM}). We then compared the course of the UPEC pathogenic cycle in Rag 1$^{-/-}$ mice and Rag 1$^{-/-}$/Atg16L1^{HM} mice that lack an intact adaptive immune system but have either an intact innate immune system (Rag1$^{-/-}$ mice) or Atg16L1^{HM} innate immune system (Rag1$^{-/-}$/Atg16L1^{HM} mice). Whereas Rag1$^{-/-}$ mice exhibited chronic bacteriuria, Rag1$^{-/-}$/Atg16L1^{HM} mice were more efficient in clearing infection as evidenced by significantly lower urine bacterial titers 7 (P < 0.05) and 14 (P < 0.01) dpi (Fig. S8). Thus, our data suggest that, in the absence of an intact adaptive immune system, the Atg16L1^{HM} innate immune system is sufficient to lower the bacterial load.

Innate immune cells, particularly macrophages and neutrophils, constitute an early line of defense against UPEC infection in vivo (25). We reasoned that Atg16L1 deficiency in these cells might contribute to the observed fast clearance of bacteriuria. This clearance could be achieved by increased recruitment of the innate immune cells to the bladder lumen to clear infection in Atg16L1^{HM} mice, and/or increased proinflammatory cytokine expression by Atg16L1^{HM} innate immune cells. We tested these hypotheses as follows. First, we examined the urines of Atg16L1^{HM} mice at acute stages of infection (6 and 24 hpi) and found that urines from Atg16L1^{HM} mice contained significantly higher numbers of neutrophils (Fig. 4*A*, 6 hpi) and monocytes on infection (Fig. 4*B*, 24 hpi). Next, we determined the proinflammatory cytokine response to infection in Atg16L1^{HM} mice. We conducted quantitative RT-PCR assays of bladder tissues as well as Bioplex assays of sera from infected control and Atg16L1^{HM} mice. We found significant increases in tissue IL-6 mRNA levels (Fig. 4*C*) (P < 0.05) and serum IL-1α levels 6 hpi (Fig. 4*D*) (P < 0.01) in Atg16L1^{HM} mice relative to control mice that were not noted before infection (Fig. S9). Together, our data show that Atg16L1 deficiency in the innate immune compartment is associated with increased recruitment of innate immune cells and a more robust proinflammatory response to infection.

To further dissect the role for autophagy protein deficiency in innate immune cells during a UTI, we used a mouse model that we previously generated (Atg5$^{fl/fl}$-Lyz-Cre mice, which are deficient in the autophagy protein Atg5 specifically in macrophages and granulocytes) (39). We evaluated Atg5 in this system, because Atg5 is an essential autophagy protein that forms a part of the Atg16L1-containing protein complex essential for autophagy (1). Consistent with Atg16L1 deficiency in immune cells causing enhanced clearance of infection, the Atg5$^{fl/fl}$-Lyz-Cre mice also resolved bacteriuria more rapidly than controls by 3 dpi (Fig. 4*E*) (P < 0.05). Furthermore, bladders of Atg5$^{fl/fl}$-Lyz-Cre mice did not exhibit evidence of organelle congestion or aberrant uroplakin receptor expression in the epithelium (Fig. S10). Thus, Atg5 protein deficiency in macrophages and granulocytes resulted in enhanced control of bacterial infection without indirect effects on the epithelium.

Together, our data show that Atg16L1 deficiency specifically in innate immune cells is the mechanism of enhanced clearance of bacteria from the urine. Atg16L1 deficiency is associated with increased recruitment of innate immune cells to the infected bladders and a robust proinflammatory response, which likely modulates the rapid UPEC clearance in Atg16L1^{HM} mice. This response is elicited even in the absence of an adaptive immune system. Finally, deficiency of another autophagy pathway protein, Atg5, exclusively in innate immune cells is sufficient to induce rapid UPEC clearance.

Discussion

Autophagy has been recognized as an important defense system to combat intracellular pathogens and hitherto, considered to play an antipathogenic role. Here, we use an in vivo model of a common infectious disease and describe a propathogen role for an

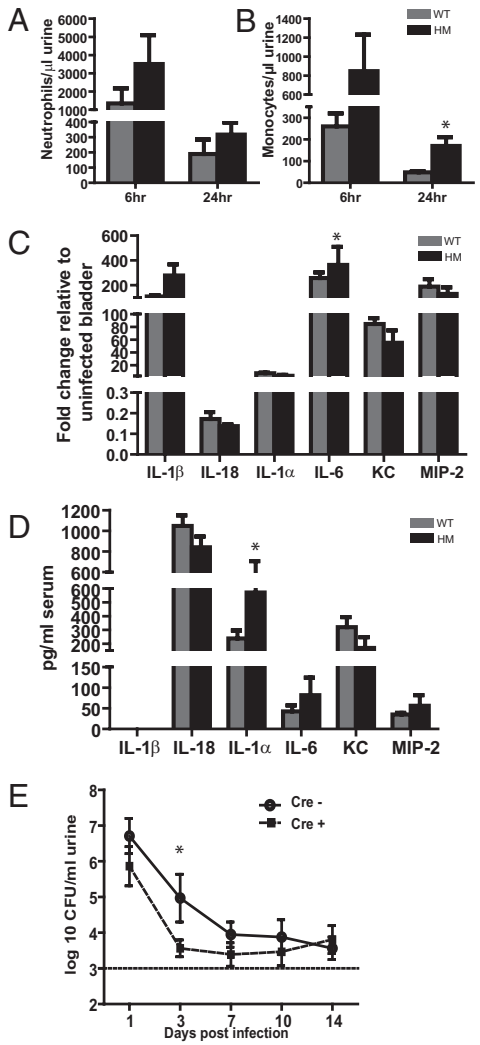

Fig. 4. Deficiency in Atg16L1 or Atg5 specifically in innate immune cells is necessary and sufficient for increased bacteriuric clearance. (*A*) Neutrophil counts in the urine. Bars represent mean ± SEM; n = 4–5 mice per time point, and n = 3 experiments. (*B*) Monocyte counts in the urine. Bars represent mean ± SEM. n = 4–5 mice per time point, and n = 2 experiments. $^*P < 0.05$ by unpaired two-tailed t test. (*C*) Quantification of bladder tissue cytokines mRNA levels by quantitative PCR at 6 hpi indicating a significant increase in IL-6 in HM compared with WT bladders. n = 3 mice/genotype. Bars represent mean ± SEM. $^*P < 0.05$ by unpaired two-tailed t test. (*D*) Quantification of serum cytokine levels by Bioplex bead array at 6 hpi showing a significant increase in IL-1α in HM compared with WT mice. n = 4–9 mice/genotype. Bars represent mean ± SEM. $^*P < 0.05$ by unpaired two-tailed t test. (*E*) CFU counts at 1–14 dpi indicating faster clearance in $Atg5^{fl/fl}$-Lyz-Cre+ compared with $Atg5^{fl/fl}$-Lyz-Cre- mice. n = 13–18 mice per time point per genotype. $^*P < 0.05$ by two-way ANOVA with Bonferroni posttest as unadjusted P values.

autophagy protein. We show that deficiency in the key autophagy protein, Atg16L1, can confer protection against a nonobligate intracellular pathogen, UPEC, which causes recurrent UTIs and has been shown to have both intracellular and extracellular stages in its pathogenic cycle. $Atg16L1^{HM}$ mice clear bacteriuria faster and renew their epithelial barrier faster. We show that this protection is mainly caused by effects of Atg16L1 deficiency in hematopoietic cells and specifically, macrophages and neutrophils that are the main cellular drivers of the fast clearance of bacteriuria. Our findings suggest the presence of a more potent innate immune system in $Atg16L1^{HM}$ mice with substantially increased proinflammatory cytokine expression as well as increased recruitment of innate immune cells to infected $Atg16L1^{HM}$ bladders. We have previously showed enhanced transcription of proinflammatory cytokines and adipokines in Paneth cells of $Atg16L1^{HM}$ mice (11). Recently, the work by Lee et al. (14) delineated that Atg16L1 expression restricts IL-1β signaling cascades and the subsequent inflammatory response, such as IL-6 production, by constitutive autolysosomal and proteosomal degradation of p62; thus, the absence of Atg16L1 leads to a hyperinflammatory response. In the setting of Crohn's disease, Atg16L1 deficiency induces elevated proinflammatory cytokine levels, and the presence of commensal bacteria leads to intestinal pathology (12). In the Atg16L1-deficient urinary tract, however, the elevated proinflammatory cytokine levels may have a beneficial effect—to better combat UPEC infection. We speculate that the more effective innate immune compartment in $Atg16L1^{HM}$ mice may promote rapid elimination of bacteria, which may prevent additional bacterial invasion into underlying urothelial cells and result in faster clearance of bacterial load (23, 24, 40), leading to restoration of a normal urothelium (41). UPEC has been shown previously to inhibit proinflammatory cytokine production after invasion into epithelial cells (23). Loss of Atg16L1 may impact the ability of UPEC to dampen the innate immune response resulting in the enhanced clearance. Together, our data all point to a protective role for the Atg16L1-deficient innate immune compartment in UTI.

Complex membrane recycling events in superficial urothelial cells play an important role in UPEC pathogenesis. Atg16L1 deficiency was associated with striking abnormalities in the accumulation of multivesicular bodies, lysosomes, and Up1a receptor in $Atg16L1^{HM}$ mice—all components of the epithelial cells that UPEC interacts with during infection. These abnormalities seem intrinsic to the Atg16L1-deficient epithelial cells, because autophagy protein deficiency in hematopoietic cells does not generate these abnormalities; these defects are found even in newly regenerated superficial cells. To our surprise, early invasion and colonization of the bladder were not dramatically altered by the Atg16L1 deficiency-induced urothelial ultrastructural changes. Strikingly, however, in the presence of these abnormalities, or perhaps because of them, UPEC seems less able to occupy the intracellular niches to persist within the urothelium as QIRs. Thus, our findings suggest that UPEC may subvert Atg16L1 and possibly other autophagy proteins to establish latency. Recent in vitro evidence supports our model. For example, the work by Starr et al. (42) showed in vitro that *Brucella* subverts autophagy complexes to facilitate its intracellular cycle and showed that *Brucella* selectively co-opts autophagy initiation complexes to subvert host clearance and promote infection.

Our findings using the hypomorphic Atg16L1 mouse model reveal a striking benefit of Atg16L1 deficiency and suggest that deficiency in an autophagy gene that can promote inflammatory disease also protects against acute UTIs. This finding leads us to speculate that *ATG16L1* allelic variants in the human population or other variants in autophagy-associated genes might be under positive selection for their ability to protect from UTIs.

Delineating mechanisms of intracellular persistence during a UTI is critical to developing effective strategies for preventing recurrent UTIs. Traditional antibiotics are unable to penetrate bladder epithelial barriers, and therefore, bacteria sequestered in QIRs can survive long term in protected niches. In addition, antibiotic therapy itself risks driving the pathogens into quiescence (43). Targeting and eliminating the small but significant intracellular pool of bacteria may have substantial clinical benefits to combat refractory and recurrent UTIs. Thus, our model provides a system for investigating the role for autophagy proteins in pathogenesis of bacterial infection in vivo and may have significant clinical implications for understanding the etiology of recurrent UTIs and providing cellular targets for therapeutic intervention.

Materials and Methods

Mice. Experiments were performed using protocols approved by the animal studies committee of the Washington University School of Medicine (Animal Welfare Assurance A-3381-01). The Atg16L1 HM2 strain ($Atg16L1^{HM}$) and

Atg16L1 heterozygote mice were generated as described (11). $Atg5^{fl/fl}$-Lyz-Cre mice were generated as described (39).

Bacterial Strains, Mouse Inoculations, and Urinalysis. UTI89, a pathogenic UPEC strain (27, 37), was used for all studies. Adult female mice (8–10 wk old) were anesthetized and inoculated transurethrally with 10^7 cfu UTI89 in PBS. Urinalysis and bacterial titering were performed as described (22, 36).

Histochemical, Immunofluorescence, and Immunoblotting Analyses. These were performed as described (11, 37). See *SI Materials and Methods*.

QIR Quantification. Six separate 5-μm serial sections over a thickness of 300 μm were immunostained with antibodies against *E. coli*, Lamp1, and E-cadherin. The total number of Lamp1 + UPEC reservoirs was imaged at 63× oil on the Zeiss scope and quantified per bladder (n = 6 sections/bladder, n = 38–40 mice/genotype).

TEM. The whole bladder was processed as described before. The number of lysosomes or MVBs was normalized to total surface area (n = 33 TEM sections, n = 3 WT, $Atg16L1^{HM}$, and bone marrow chimeric mice).

Bioplex Cytokine Bead Array Assay. Sera were obtained before infection and at 6 hpi, and cytokine levels were measured using Bioplex kit (BioRad) (44).

Neutrophil and Monocyte Counts in Urine. The urines were collected before and after infection, and neutrophil and monocyte counts were analyzed using HEMAVET 950, Veterinary 5 part WBC Hematology System (Drew Scientific, Dallas, TX).

Bone Marrow Chimera Generation. Seven-week-old recipients received 1,000 Gy γ-irradiation in divided doses over 2 sequential d and were injected i.v. with 1×10^7 T lymphocyte-depleted bone marrow cells from sex-matched donors. Mice were allowed 8 wk for reconstitution before use for experiments (24), and then, they were UPEC-infected. The urine bacterial titers were examined at 0–14 d. Appropriate reconstitution of lymphocyte compartments was examined by flow cytometry at the time of sacrifice.

Statistical Analysis. To assess the significance of a difference between groups, a two-sample, unpaired t test was performed using Graph Prism software. For time-course studies, the SE used in t test was estimated by ANOVA, and two-sample tests were performed at individual time points. To control for false positives, Bonferroni adjusted P values at individual time points are reported. A P value less than 0.05 (*) was considered to be significant, a P value less than 0.01 (**) was considered to be very significant, and a P value less than 0.001 (***) was considered to be extremely significant.

ACKNOWLEDGMENTS. We thank members of our laboratory and Dr. Jason Mills for comments. We thank Dr. Wojtech Swat for helping with irradiation studies and Dr. Wandy Beatty for TEM. This work was funded by National Institute of Child Health and Human Development Grant T32-54560 (to G.R.M.), U54AI057160, Project 5 (to H.W.V.), and K99/R00 Pathway to Independence Award DK080643 (to I.U.M). K.C. is an Allege Easel Wall Fellow of the Damon Runyon Cancer Research Foundation.

1. Levine B, Mizushima N, Virgin HW (2011) Autophagy in immunity and inflammation. *Nature* 469:323–335.
2. Virgin HW, Levine B (2009) Autophagy genes in immunity. *Nat Immunol* 10:461–470.
3. Deretic V, et al. (2009) Autophagy in immunity against mycobacterium tuberculosis: A model system to dissect immunological roles of autophagy. *Curr Top Microbiol Immunol* 335:169–188.
4. Levine B, Kroemer G (2009) Autophagy in aging, disease and death: The true identity of a cell death impostor. *Cell Death Differ* 16:1–2.
5. Saitoh T, et al. (2008) Loss of the autophagy protein Atg16L1 enhances endotoxin-induced IL-1beta production. *Nature* 456:264–268.
6. Orvedahl A, Levine B (2009) Eating the enemy within: Autophagy in infectious diseases. *Cell Death Differ* 16:57–69.
7. Orvedahl A, et al. (2010) Autophagy protects against Sindbis virus infection of the central nervous system. *Cell Host Microbe* 7:115–127.
8. Campoy E, Colombo MI (2009) Autophagy subversion by bacteria. *Curr Top Microbiol Immunol* 335:227–250.
9. Deretic V (2010) Autophagy in infection. *Curr Opin Cell Biol* 22:252–262.
10. Noda T, Yoshimori T (2009) Molecular basis of canonical and bactericidal autophagy. *Int Immunol* 21:1199–1204.
11. Cadwell K, et al. (2008) A key role for autophagy and the autophagy gene Atg16l1 in mouse and human intestinal Paneth cells. *Nature* 456:259–263.
12. Cadwell K, et al. (2010) Virus-plus-susceptibility gene interaction determines Crohn's disease gene Atg16L1 phenotypes in intestine. *Cell* 141:1135–1145.
13. Plantinga TS, et al. (2011) Crohn's disease-associated ATG16L1 polymorphism modulates pro-inflammatory cytokine responses selectively upon activation of NOD2. *Gut* 60:1229–1235.
14. Lee J, et al. (2012) Autophagy suppresses interleukin-1β (IL-1β) signaling by activation of p62 degradation via lysosomal and proteasomal pathways. *J Biol Chem* 287: 4033–4040.
15. Franke A, et al. (2010) Genome-wide meta-analysis increases to 71 the number of confirmed Crohn's disease susceptibility loci. *Nat Genet* 42:1118–1125.
16. Hampe J, et al. (2007) A genome-wide association scan of nonsynonymous SNPs identifies a susceptibility variant for Crohn disease in ATG16L1. *Nat Genet* 39(2): 207–211.
17. Dielubanza EJ, Schaeffer AJ (2011) Urinary tract infections in women. *Med Clin North Am* 95:27–41.
18. Foxman B (2010) The epidemiology of urinary tract infection. *Nat Rev Urol* 7: 653–660.
19. Anderson GG, et al. (2003) Intracellular bacterial biofilm-like pods in urinary tract infections. *Science* 301:105–107.
20. Zhou G, et al. (2001) Uroplakin Ia is the urothelial receptor for uropathogenic Escherichia coli: Evidence from in vitro FimH binding. *J Cell Sci* 114:4095–4103.
21. Garofalo CK, et al. (2007) Escherichia coli from urine of female patients with urinary tract infections is competent for intracellular bacterial community formation. *Infect Immun* 75:52–60.
22. Rosen DA, Hooton TM, Stamm WE, Humphrey PA, Hultgren SJ (2007) Detection of intracellular bacterial communities in human urinary tract infection. *PLoS Med* 4(12): e329.
23. Hunstad DA, Justice SS, Hung CS, Lauer SR, Hultgren SJ (2005) Suppression of bladder epithelial cytokine responses by uropathogenic Escherichia coli. *Infect Immun* 73: 3999–4006.
24. Schilling JD, Martin SM, Hung CS, Lorenz RG, Hultgren SJ (2003) Toll-like receptor 4 on stromal and hematopoietic cells mediates innate resistance to uropathogenic Escherichia coli. *Proc Natl Acad Sci USA* 100:4203–4208.
25. Ragnarsdottir B, Lutay N, Gronberg-Hernandez J, Koves B, Svanborg C (2011) Genetics of innate immunity and UTI susceptibility. *Nat Rev Urol* 8:449–468.
26. Hunstad DA, Justice SS (2010) Intracellular lifestyles and immune evasion strategies of uropathogenic Escherichia coli. *Annu Rev Microbiol* 64:203–221.
27. Mysorekar IU, Hultgren SJ (2006) Mechanisms of uropathogenic Escherichia coli persistence and eradication from the urinary tract. *Proc Natl Acad Sci USA* 103: 14170–14175.
28. Bishop BL, et al. (2007) Cyclic AMP-regulated exocytosis of Escherichia coli from infected bladder epithelial cells. *Nat Med* 13:625–630.
29. Song J, Bishop BL, Li G, Duncan MJ, Abraham SN (2007) TLR4-initiated and cAMP-mediated abrogation of bacterial invasion of the bladder. *Cell Host Microbe* 1: 287–298.
30. Guo X, et al. (2009) Involvement of vps33a in the fusion of uroplakin-degrading multivesicular bodies with lysosomes. *Traffic* 10:1350–1361.
31. Khandelwal P, Abraham SN, Apodaca G (2009) Cell biology and physiology of the uroepithelium. *Am J Physiol Renal Physiol* 297:F1477–F1501.
32. Kreft ME, Jezernik K, Kreft M, Romih R (2009) Apical plasma membrane traffic in superficial cells of bladder urothelium. *Ann N Y Acad Sci* 1152:18–29.
33. Sun TT, Liang FX, Wu XR (1999) Uroplakins as markers of urothelial differentiation. *Adv Exp Med Biol* 462:7–18.
34. Birmingham CL, et al. (2007) Listeria monocytogenes evades killing by autophagy during colonization of host cells. *Autophagy* 3:442–451.
35. Zheng YT, et al. (2009) The adaptor protein p62/SQSTM1 targets invading bacteria to the autophagy pathway. *J Immunol* 183:5909–5916.
36. Hung CS, Dodson KW, Hultgren SJ (2009) A murine model of urinary tract infection. *Nat Protoc* 4:1230–1243.
37. Mysorekar IU, Isaacson-Schmid M, Walker JN, Mills JC, Hultgren SJ (2009) Bone morphogenetic protein 4 signaling regulates epithelial renewal in the urinary tract in response to uropathogenic infection. *Cell Host Microbe* 5:463–475.
38. Mombaerts P, et al. (1992) RAG-1-deficient mice have no mature B and T lymphocytes. *Cell* 68:869–877.
39. Zhao Z, et al. (2008) Autophagosome-independent essential function for the autophagy protein Atg5 in cellular immunity to intracellular pathogens. *Cell Host Microbe* 4:458–469.
40. Horvath DJ, Jr., et al. (2011) Morphological plasticity promotes resistance to phagocyte killing of uropathogenic Escherichia coli. *Microbes Infect* 13:426–437.
41. Mysorekar IU, Mulvey MA, Hultgren SJ, Gordon JI (2002) Molecular regulation of urothelial renewal and host defenses during infection with uropathogenic Escherichia coli. *J Biol Chem* 277:7412–7419.
42. Starr T, et al. (2012) Selective subversion of autophagy complexes facilitates completion of the Brucella intracellular cycle. *Cell Host Microbe* 11:33–45.
43. Blango MG, Mulvey MA (2010) Persistence of uropathogenic Escherichia coli in the face of multiple antibiotics. *Antimicrob Agents Chemother* 54:1855–1863.
44. Hannan TJ, Mysorekar IU, Hung CS, Isaacson-Schmid ML, Hultgren SJ (2010) Early severe inflammatory responses to uropathogenic E. coli predispose to chronic and recurrent urinary tract infection. *PLoS Pathog* 6:e1001042.